'Near-field effects in parametric end-fire arrays'

H. O. Berktay

Electronic & Electrical Engineering Department,
University of Birmingham

1. Introduction

Since Westervelt's proposal [1] that non-linear interaction between two coincident acoustic waves be used to generate highly directional waves at a low-frequency, the results of a number of experiments have been published.[2-6] The experimental results tend to confirm Westervelt's basic suggestion that the scattered interaction frequency waves can exist independently of the transmitted primary waves and that they are highly directional. However, with perhaps two exceptions, the experiments indicate that the difference-frequency beams are more directional than estimated by Westervelt on Rutherford scattering basis, assuming that the primary beams have negligible cross-sectional dimensions and that the observer is in the far-field of the parametric array. One possible explanation[7,8] put forward was that an "aperture effect" must be taken into consideration when estimating the directivity pattern of the difference frequency waves when the interaction volume is substantially limited to the near field of the projector by the rate of absorption of the primary waves. Although some of the experimental results can be explained by the inclusion of this aperture factor, some other results have other features which need explaining. For example, Smith's results (reference 3b, Fig.4) showed that the measured beamwidth at the difference frequency was substantially lower than the estimated value, almost independently of the frequency.

In this paper, two possible causes of such phenomena are investigated. These are the possible effects on the measured directivity patterns due to interactions occurring in the Fresnel region of the projector and those due to the observer not being at a sufficiently great distance from the interaction region. Only the case of a square piston will be considered.

2. Source distribution in the near-field of a square piston

The acoustic pressure produced by transmission from a piston in an infinite baffle can be represented in the form [9]

$$p = j\,(\rho c_o U/\lambda)\,\exp\,(j\omega t)\iint_s \left[\exp(-jkr)/r\right]ds \qquad \ldots (1)$$

where $\underline{U}$ is the amplitude of the velocity of the piston, k is the wave-number and λ the wavelength in the medium, and the double integral is evaluated over the surface of the piston. Here, r is the distance between the observer at (x,y,z) and an elemental area on the surface of the piston at (0, y_1,z_1), the piston surface being assumed to lie in the plane x = o. Then, by substituting $\frac{1}{R}$ for $\frac{1}{r}$, and

$$r \doteq x\left(1+\frac{y_o^2+z_o^2}{2x^2}\right)$$

in the phase term in the integrand, the pressure can be calculated[9] in the phasor form as

$$\underline{P} = (j\rho_o c_o \underline{U}/2) \quad \exp(-jkx) \int_{g_1}^{g_2} \exp(-\frac{j\pi g^2}{2})dg$$

$$\times \int_{h_1}^{h_2} \exp(-\frac{j\pi}{2} h^2)dh \qquad \ldots(2)$$

where $y_o = y - y_1$, $z_o = z - z_1$,

$g = a\, y_o$, $h = a\, z_o$,

$g_1 = a(y-b)$, $h_1 = a\,(z-b)$

$g_2 = a(y+b)$, $h_2 = a\,(z+b)$

and $a = \sqrt{2/\lambda x}$

Freedman showed[9] that the approximations made in the substitutions for r were valid in the immediate vicinity of the transducer. In his derivation of $\underline{P}$ a factor $\cos\gamma = x/R$ is also included. Here, this is ignored as we are working with small angles of γ (again, except in the immediate vicinity of the piston). Throughout this treatment we also make use of Freedman's conclusion that, within the near-field, $\underline{P}$ rapidly reduces to zero as y or z becomes greater than b.

The coefficient of the integrals in equation (2) represents a plane wave propagating in the x direction. The integrals will be denoted by F(y) and F(z) respectively, where

$$F(y) = f\left[a\,(y-b)\right] - f\left[a\,(y+b)\right]$$

and $f(m)$ is the Fresnel integral,

i.e. $$f(m) = \int_0^m \exp(-\frac{j\pi}{2} v^2)\, dv$$

If two waves at frequencies ω_1 and ω_2 are launched from the piston simultaneously,

$$\underline{P_1} = (j\rho_o c_o \underline{U_1}/2) \exp(-jk_1 x) \cdot F_1(y) \cdot F_1(z)$$

and

$$\underline{P_2} = (j\rho_o c_o \underline{U_2}/2) \exp(-jk_2 x) \cdot F_2(y) \cdot F_2(z) \qquad \ldots(3)$$

(Here, subscripts 1 and 2 are used to indicate that the corresponding frequencies refer).

Then, the low-frequency source function at point (x, y, z) is determined by the product $\underline{P_1}\,\underline{P_2^*}$, where the asterisk indicates the complex conjugate of the quantity. Including the absorption terms, one can write,

$$\underline{Q_v} = \exp\left[(-\alpha_1 + \alpha_2 + j(k_1 - k_2))x\right]$$

$$\cdot F_1(z) \cdot F_2^*(z) \cdot F_1(y) \cdot F_2^*(y) \qquad \ldots(4)$$

If this expression is integrated for all y and z, an expression is obtained for the linear distribution of the low-frequency sources. This amounts to reducing the interaction problem to one of infinitesimal cross-section, similar to that considered by Westervelt[1]. Hence, the aperture effect[7,8] would have to be taken into account separately.

As F(z) vanishes rapidly for |z|>b, the product of two such functions will tend to zero even more rapidly. Similar considerations apply for F(y). Hence, the integrals with respect to y and z are taken between $-\infty$ and $+\infty$.

i.e. $\underline{Q_s}(x) = \iint_{-\infty}^{\infty} Q_v \, dy \, dz$

i.e. $\propto \exp\left[-(\alpha_1 + \alpha_2 + jk_-)x\right]$

$$\cdot \int_{-\infty}^{\infty} F_1(y) \cdot F_2^*(y) \cdot dy \cdot \int_{-\infty}^{\infty} F_1(z) \cdot F_2^*(z) \cdot dz \qquad \ldots(5)$$

Because of symmetry, the two integrals are equal. Thus, only the integral

$$\int_{z=-\infty}^{\infty} F_1(z) \cdot F_2^*(z) \cdot dz$$ needs to be evaluated.

By changing the variables and the order of integration (which is permissible as F(z) is a well-behaved function) an expression is obtained for $\underline{Q_s}(x)$ in the form

$$\underline{Q_s}(x) \propto \exp\left[(-\alpha_1 + \alpha_2 + jk_-)x\right] \frac{\pi x c_0}{\omega_2} I^2 \qquad \ldots(6)$$

where I is given by

$$I = 2\left(\omega_1 - \omega_2/\omega_1\right)^{1/2} \int_{v=0}^{V} f^*(v) \cdot dv, \qquad \ldots(7)$$

$$f^*(v) = \int_0^v \exp\left(j\frac{\pi}{2}t^2\right) dt$$

and $$V = 2b\left[\omega_1\omega_2/\pi x c_0 (\omega_1 - \omega_2)\right]^{1/2}$$

As v is real, I can be separated into its real and imaginary parts, and I^2 can be evaluated.

If V is large, the asymptotic value of the Fresnel integrals (i.e. C(v) = S(v) = 1/2) can be used, which yields

$$(\pi x c_0/\omega_2) I^2 \doteq 8b^2 j \qquad \ldots(8)$$

Substitution in (6) gives the linear source function used by Westervelt[1], which results in Rutherford scattering for the difference-frequency waves.

Using tables of Fresnel integrals, I was computed numerically for various values of W, and (for the range of W of interest) and approximate expression was developed, with an error not exceeding about 3% in the worst case. Using this expression, it was found that

$$(\pi x c_o/\omega_2) \quad I^2 \doteq 8b^2 j \left[1 + j\, 0.204\, B_o^2\, x - 0.64\, B_o \sqrt{x}(1+j)\right] \qquad \ldots(9)$$

Here $B_o^2 = (\omega_1 - \omega_2)/8\omega_2 R_{f_1}$,

where $R_{f_1} = b^2/\lambda_1$, i.e. the Fresnel distance at frequency ω_1.

Using equations (9) and (6) the far-field radiation pattern at the difference-frequency can be calculated in closed form. We obtain the pressure at an angular position θ,

$$P_-(\theta) \propto \frac{j}{2\beta} + \frac{0.283\, B_o(1 - j)}{\beta^{3/2}} - \frac{0.102\, B_o^2}{\beta^2} \qquad \ldots(10)$$

where $\beta \doteq (\alpha_1 + \alpha_2 - \alpha_-) + jk_-\,(1-\cos\theta)$, ...(10a)

and, for small θ, reduces to

$$\beta \doteq (\alpha_1 + \alpha_2 - \alpha_-)\;(1 + j\,\phi^2), \qquad \ldots(10b)$$

$\phi = \theta / \theta_d$, θ_d being half the 3 db beamwidth in the case of Rutherford scattering

i.e. $\theta_d^2 = 2\,(\alpha_1 + \alpha_2 - \alpha_-)/k_-$.

Pressure level along the axis can be calculated by putting $\theta = \phi = o$ in expression 10. Then, the directivity pattern can be calculated as

$$D\,(\theta) = P_-(\theta) / P_-(o) \;. \qquad \ldots(11)$$

$P_-(o)$ and $D\,(\theta_d)$ were evaluated for the parameters of Smith's experiment[3], which were:-

centre frequency 2.85 MHz, 2b = 3cm, R = 5 m.

The results are shown in Table 1. Calculations for other values of θ showed a similar pattern. In other words, the effect of the interaction being in the near-field of a transducer causes a small, general reduction in the difference frequency pressure (which depends on the difference frequency), but affects the beamwidth only marginally. This variation in the directivity pattern is far too small to explain the deviations observed in the experiment.

3. The near-field of a continuous end-fire-array with exponential amplitude taper

Using the conclusions of the previous section, it should be possible to estimate parametric end-fire effects by assuming Westervelt's original model of a line-array with exponential taper, additionally including an "aperture factor", where applicable, even when interaction takes place in the Fresnel region. In the analysis offered in this section, the aperture factor is neglected - it can be incorporated into the results.

The geometry considered is shown in Fig. 2. A line array with exponential taper is assumed tobe along the x - axis. The linear density of source is given by

$$q = Q_o \exp(j\omega_- t) \exp\left[-(\alpha_1 + \alpha_2 + jk_-)\,x\right] \qquad \ldots(12)$$

Then, the difference-frequency pressure at point (R.Θ) will be proportional to

$$\underline{S}(R, \Theta) = \int_x \frac{1}{r} \exp\left[-(\alpha_1 + \alpha_2 + j\underline{k})\,x - (\alpha_- + jk_-)r\right].\,dx \qquad (13)$$

As $R \to \infty$, this gives Westervelt's result, which in the notation used becomes

$$\underline{S}(R,\Theta) = \exp\left[-\alpha_- + jk_-)\,R\right] / R\beta \qquad \ldots(14)$$

where β is given in equation (10a). This development relies on the use of the approximation $r \doteq R - x\cos\Theta$ and then integration for x between 0 and ∞.

If $R >> 1/(\alpha_1 + \alpha_2)$, as a second approximation,

$$r = R - x\cos\Theta + (x^2/2R)\sin^2\Theta \qquad \ldots(15)$$

It can be shown that for small $|\Theta|$, the variation in the amplitude term 1/r with x producesa change in the radiated pressure level, but causes only minor effects in the directivity pattern. Hence, for the present purposes, we replace equation (13) by

$$\underline{S}(R,\Theta) \doteq \exp\left[-(\alpha_- + jk_-)\right]/R \int_x \exp(-\beta x - \gamma x^2)\,dx \qquad \ldots(13a)$$

where $\gamma = (\alpha_- + jk_-)\sin^2\Theta / 2R$. Integrating for

$$o < x < \infty,$$

$$\underline{S}(R,\Theta) \doteq L(z)\ \exp\left[-(\alpha_- + jk_-)\,R\right] / R\beta \qquad \ldots(16)$$

where

$$z = \left[(\alpha_1 + \alpha_2 - \alpha_-)R/8\right]^{1/2}\left[\phi + 1/\phi + j(\phi - 1/\phi)\right]$$

and $L(z) = \sqrt{\pi}\ z\ \exp z^2 \,.\, \text{erfc}\ z,$ $\qquad \ldots(17)$

$$\text{erfc}\ z = 2/\sqrt{\pi} \int_{u=z}^{\infty} \exp(-u^2)\,du, \text{ and as above } \phi = \Theta/\Theta_d.$$

For $\Theta = \phi = o$, equation (13a) gives

$$\underline{S}(R,0) \doteq \exp\left[-(\alpha_- + jk_-)\,R\right] \big/ (\alpha_1 + \alpha_2 - \alpha_-)R \qquad \ldots(18)$$

Hence, the normalized directivity function at range R can be written (from equations 16, 18 and 10b) in the form

$$D(R, \theta) = |L(z)| \cdot D(\infty, \theta) \qquad \ldots(19)$$

where $$D(\infty, \theta) = 1 / |1 + j\phi^2| .$$

z is a complex quantity, depending solely on the normalized angle ϕ and the attenuation term $M = (\alpha_1 + \alpha_2 - \alpha_-')R$.

In the computation of error functions with complex arguments a useful auxiliary function, $w(jz)$, is tabulated [10]

where $$w(jz) = \exp z^2 \cdot \text{erfc } z \qquad \ldots(20)$$

Then,

$$D(R, \theta) = \sqrt{\pi} \cdot |z| \cdot |w(jz)| \;/\; (1 + \phi^4)^{1/2} \qquad \ldots(21)$$

Clearly, $D(R, \theta)$ can be calculated as a function of ϕ for various values of the attenuation term M.

$L(z)$ for three values of M, as well as $D(\infty, \theta)$, are shown in Fig.3 as functions of ϕ. The correction term $20 \log |L(z)|$ becomes negligible for small and large values of ϕ. It is also reduced as M becomes large.

Comparison with experimental results

In one of Smith's experiments, a 3.0 cm square transducer was used to transmit two primary waves with a centre frequency of about 2.85MHz. Directivity patterns were measured at a range of 5.0 m. The corresponding value of M was 2.6 Nepers, and that of the Fresnel distance about 45 cm. His results at various difference frequencies are shown in Fig.4, plotted here against normalised angle ϕ, the value of θ_d used being that calculated for each frequency. The Rutherford scattering curve, and that corrected using the results of Fig. 3 are also shown. The following comments appear to be in order.

(i) At the difference frequencies considered, the aperture effect can be neglected. (In any case, it appears somewhat doubtful as to whether the aperture factor should be used in this experiment as the interaction volume is not confined to the Fresnel region).

(ii) The grouping of the experimental results when plotted against normalized angle is good.

(iii) For smaller values of ϕ the corrected directivity pattern agrees very well with experimental results, but the results diverge for large values of ϕ.

In Fig. 5, Smith's results showing 3dB beamwidth as a function of the difference frequency are reproduced, together with the corresponding values calculated from $D(\infty, \theta)$ and from $D(R,\theta)$. The agreement between the computed results on the basis of the analysis presented in this section and the experimental results is very encouraging.

H.M. Merklinger has kindly made available some experimental results, as yet unpublished. These results were obtained at a difference frequency of 1.1 MHz, the centre-frequency of the primary waves (which were transmitted from a 1 cm square transducer) was 8.75 MHz. With absorption coefficients of about 1.8 N/m, the bulk of the interaction could be assumed to take place within the Fresnel region (about 58 cm). Therefore, the directivity patterns obtained at various ranges R were corrected for the aperture factor, and are shown plotted in Fig. 6. In the same figure, the Rutherford scattering curve and that corrected for R = 1.7 m are also shown. The agreement between the experimental results and those computed from equation 19 is again, very good. However, computations made for R = 1.1 m and for R = 65 cm fall far short of explaining the rapid narrowing of the beams at shorter ranges. This latter effect needs further investigation.

4. Conclusions

In designing an experiment with a parametric end-fire-array, the observer should be placed at as great a distance from the projector as possible. An idea of the value of R necessary for the Rutherford scattering formula to be valid can be obtained by considering an asymptotic expansion of L(z) for large values of z. It can be shown[10] that

$$L(z) = 1 - \frac{1}{2z^2} + \frac{1.3}{2^2 z^4} - \dots \qquad \dots(17a)$$

For example, at a 3dB point (i.e. for $\phi = 1$)

$$z = (M/2)^{1/2} \qquad \text{Hence,}$$

$$L(z) = 1 - \frac{1}{M} + \frac{3}{M^2}$$

Therefore, for the measured values of the 3dB beamwidth to agree with Westervelt's result (with the inclusion of the aperture effect, where appropriate) the value of the attenuation term $M = (\alpha_1 + \alpha_2 - \alpha_-)R$ must be large.

The agreement between Merklinger's experimental results and the theory confirms the need for the inclusion of the aperture factor when the bulk of the interaction takes place within the Fresnel region of the projector. The results of the analysis in section 2 suggest that the consequence of the bulk of the interaction occurring in the Fresnel region may be a slight reduction in the source level at the difference frequency, without any noticable variation in the directivity pattern.

The analysis presented here does not explain the very narrow beams obtained at much shorter ranges. This effect needs further study.

TABLE 1

Application of the results to Smith's experiment[3]

Difference freq.	$\|P_-(o)/P_-^W(o)\|$	$\|P_-(\theta_d)/P_-(o)\|$
kHz	dB	dB
100	-0.6	-3.1
300	-1.1	-3.1

$P_-^W(o)$ the axial pressure obtained from Westervelt's result.

REFERENCES

1. P.J. Westervelt 1960 J.Acoust.Soc.Am. 32, 934A
Parametric end-fire array
2. J.L.S. Bellin and R.T. Beyer 1962 J. Acoustic Soc.Am. 34,1051. Experimental investigation of an end-fire array.
3. (a) H.O. Berktay and B.V. Smith 1965 Electronics Letters 1, 6.
also
(b) B.V. Smith 1971 J. of Sound Vib. 14, 7. An experimental study of a parametric end-fire array.
4. H. Hobaek 1967 J. of Sound Vib. 6, 460. Experimental investigation of an acoustical end-fire array.
5. T.G. Muir and J.E. Blue 1969 J. Acoust,Soc. Am 46, 227. Experiments on the acoustic modulation of large amplitude waves.
6. V.A. Zverev and A.I. Kalachev 1968 Soviet Physics - Acoustics 14, 173. Measurement of the scattering of sound by sound in the superposition of parallel beams.
7. H.O. Berktay 1965 J. of Sound Vib. 2, 435. Possible exploitation of non-linear acoustics in underwater transmitting applications.
8. J. Naze and S. Tjøtta 1965 J. Acoust. Soc..Am.37, 174 Non-linear interaction of two sound beams.
9. A. Freedman 1960 J. Acoust.Soc.Am. 32, 197 Sound field of a rectangular piston.
10. For example, M. Abromowitz and I.A. Stegun (Editors) 1965 Handbook of Mathematical functions Dover Publications.

Captions for figures

Fig. 1. The geometry used for the source distribution in the vicinity of a piston.

Fig. 2. The geometry for the near-field calculations in an end-fire array.

Fig. 3. Near-field correction for normalized directivity pattern.

. . . AR = 2.6

x x x AR = 4.2

o o o AR = 7.15

- - - Rutherford Scattering Curve

Fig. 4. Comparison with Smith's experimental results - beam patterns.

———— Rutherford scattering curve

Δ Δ Δ Corrected for AR = 2.6

Experimental results at various difference frequencies:-

. . . 100 kHz, ooo 160 kHz

x x x 240 kHz

Fig. 5. Comparison with Smith's experimental results - 3 dB beamwidths.

———— For Rutherford scattering

- - - - Corrected for AR = 2.6

. . . . Various experimental results.

Fig. 6. Comparison with Merklinger's experiments

———— Rutherford scattering

- - - - Corrected for AR = 7.15 (R = 1.7)

Experimental results:-

o o o R = 1.7 m, . . . R = 1.5 m,

x x x R = 1.0 m, Δ Δ Δ R = 0.625 m.

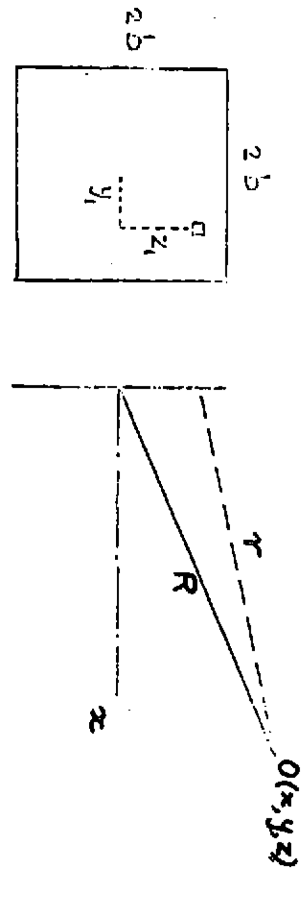

FIG. 1

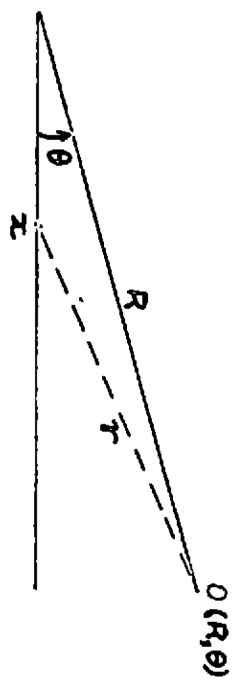

FIG. 2

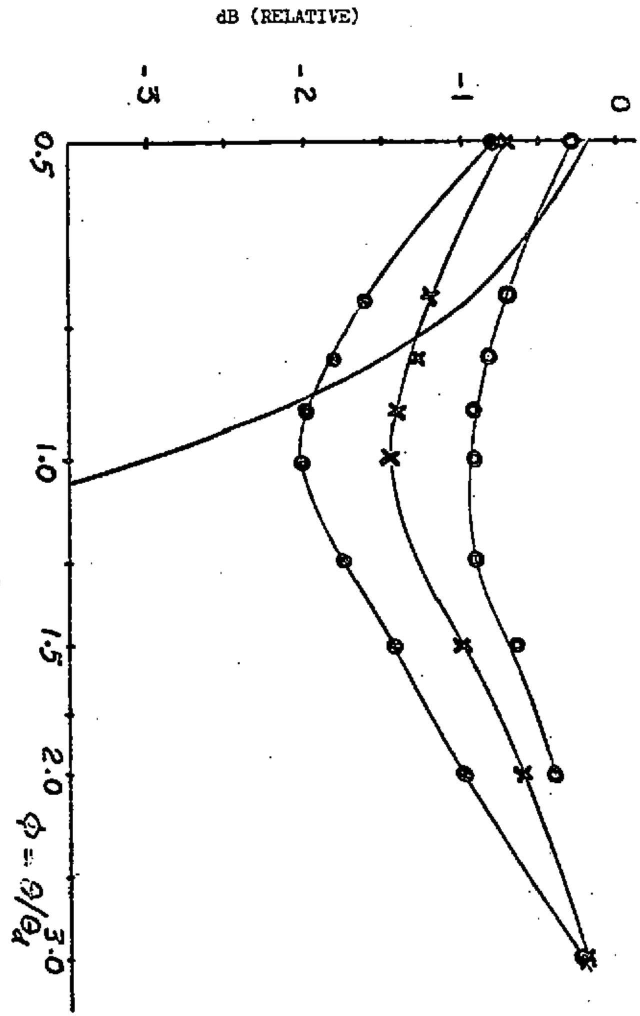

FIG. 3

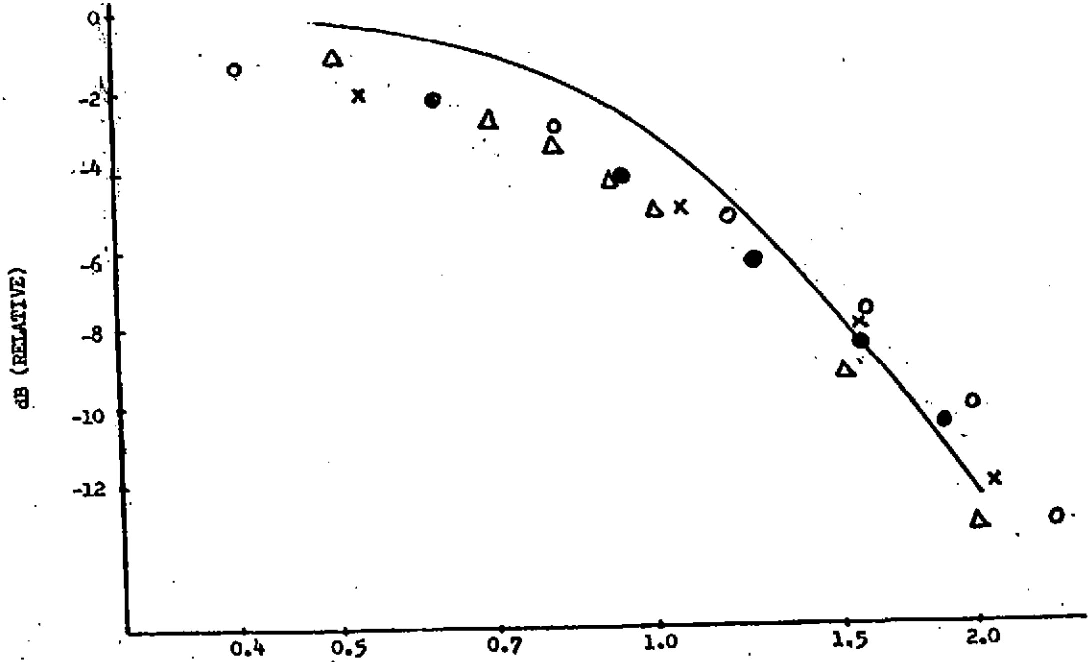

FIG. 4

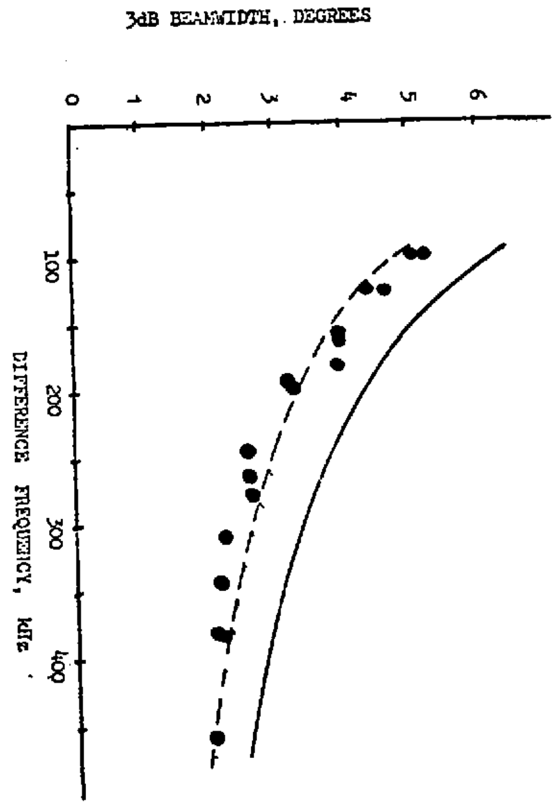
3dB BEAMWIDTH, DEGREES
0
1
2
3
4
5
6
100
200
300
400
DIFFERENCE FREQUENCY, kHz

FIG. 5

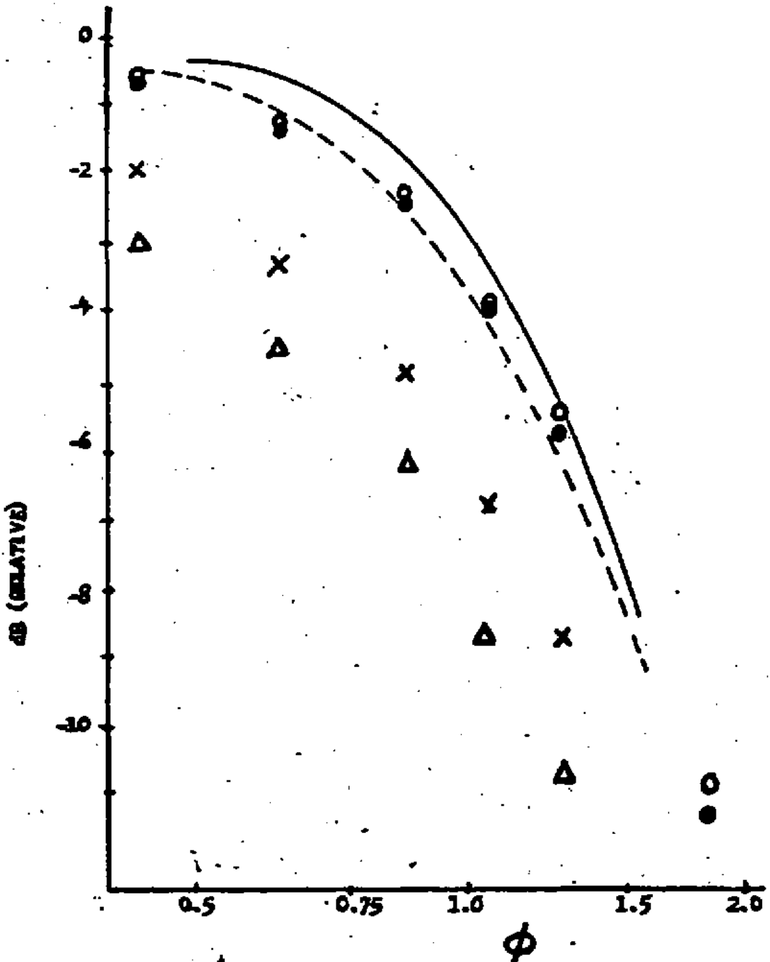

FIG. 6